MASS SPECTROGRAPH STUDY OF THE EVAPORATION OF ALKALINE EARTH CARBONATES

G. Déjardin, G. Mesnard and R. Uzan

Translation of " Etude au spectrographe de masse des produits d'évaporation de carbonates alcalino-terreux", Le Vide, Vol. 16, No. 94, July-August, 1961, pp. 157-166

NATIONAL AERONAUTICS AND SPACE ADMINISTRATION
WASHINGTON, D. C. 20546 FEBRUARY 1975

STANDARD TITLE PAGE

1. Report No.	2. Government Accession No.	3. Recipient's Catalog No.
NASA TT F-16,179		

4. Title and Subtitle	5. Report Date
MASS SPECTROGRAPHIC STUDY OF THE EVAPORATION PRODUCTS OF ALKALINE EARTH CARBONATES	MARCH 1975
	6. Performing Organization Code
7. Author(s)	8. Performing Organization Report No.
G. Déjardin, G. Mesnard and R. Uzan	10. Work Unit No.
	11. Contract or Grant No. NASw-2483
9. Performing Organization Name and Address SCITRAN Box 5456 Santa Barbara, CA 93108	13. Type of Report and Period Covered Translation
12. Sponsoring Agency Name and Address National Aeronautics and Space Administration Washington, D.C. 20546	14. Sponsoring Agency Code

15. Supplementary Notes

Translation of "Etude au spectrographe de masse des produits d'évaporation de carbonates alcaline-terreux", Le Vide, Vol. 16, No. 94, July-August, 1961, pp. 157-166.

16. Abstract

This preliminary study, undertaken after a mass spectrograph was put into service, is mainly concerned with the products that evolve at high temperature from alkaline earth carbonates utilized in the preparation of oxide cathodes. The experimental results show that it is thereby possible to obtain information on the behavior of materials in the course of formation and activation of emissive coating. For numerous ions that are produced by electron bombardment, the "evolution potentials" have been deduced from curves showing the variations in the ionic current as a function of the incident electron energies. By way of a comparison, a few gases have also been studied under the same conditions.

17. Key Words (Selected by Author(s))	18. Distribution Statement
	Unclassified - Unlimited

19. Security Classif. (of this report)	20. Security Classif. (of this page)	21. No. of Pages	22. Price
Unclassified	Unclassified	26	

MASS SPECTROGRAPH STUDY OF THE EVAPORATION OF ALKALINE EARTH CARBONATES

Georges Dejardin*, Guy Mesnard* and
Robert Uzan*

This preliminary study, undertaken after a mass spectrograph was /157** put into service, is mainly concerned with the products that evolve at high temperature from alkaline earth carbonates utilized in the preparation of oxide cathodes. The experimental results show that it is thereby possible to obtain information on the behavior of materials in the course of formation and activation of emissive coating. For numerous ions that are produced by electron bombardment, the "evolution potentials" have been deduced from curves showing the variations in the ionic current as a function of the incident electron energies. By way of a comparison, a few gases have also been studied under the same conditions.

The mass spectrograph is a convenient tool for studying products produced by a solid when heated in a vacuum. We have used this method for alkaline earth carbonates utilized in the preparation of

---

* Institute for General Physics at the University of Lyons.

** Numbers in the margin indicate pagination in the original foreign text.

oxide cathodes. Such an investigation seems capable of providing an indication of the operation of cathodes of this type. An analogous evaporation is in fact produced during the "formation" and the activation of the cathode in an electron tube. In fact, the ionization of residual gases, namely by emitted electrons, is comparable to that produced in a mass spectrograph. On the other hand, with this instrument one can detect differences in composition and behavior of the materials used: if one studies the emissive properties at the same time, it is then possible to determine the usefulness or the nefarious effects of certain impurities. We should, nevertheless, point out that in observations made with a mass spectrograph, the product is not traversed by a current, and is thus in an atmosphere that differs from that of an electron tube.

The products evolved from an oxide cathode have already been studied by Plumlee and Smith, as well as other authors [1], by means of a mass spectrograph. The results obtained in our work extend to alkaline earth dioxides which have been used in the manufacture of some cathodes.

Experimental Technique

We have at our disposal an Atlas-Werke mass spectrograph (Nier type at 60°) of classical construction. For observations of solids, we use, independently of the electron emitting filament that ionizes the evaporation products, an "ion furnace" designed to heat the material being studied. A very small quantity (on the order of a few tenths of micrograms) of the substance being studied is deposited on a tungsten filament that is heated by the joule effect. The initial adhesion of the substance on the filament is obtained by means of a thin layer of a nitrocellulose base binder. (This binder is commonly used in the fabrication of electron tubes.) We have studied only positive ions.

To interpret the results, one has to start back from the ions to the products that produced them. In general, a knowledge of the charge-to-mass ratio is not sufficient for the identification of

ions. As we will see, one can derive much information from the curves of ionic current variations as a function of incident electron energy. Also very useful is the comparison relation to isotopes.

The determination of the relative quantities of the products evolved is up against considerable difficulties. One does not, in general, know the "effective ranges" of ionization corresponding to the various radicals or molecules. We will assume that they are the same when results of this type are mentioned. Moreover, these are related to an invariant electron energy (approximately 70 eV). Other causes of uncertainty reside with the constant change in the partial pressures, resulting particularly from pumping, as well as /158 from the formation of deposits on the walls.

The carbonates that were studied are substances of some considerable purity, used, for the most part, in the industrial manufacture of electron tubes. They include simple barium carbonates, carbonates of strontium or of calcium; two co-precipitated carbonates of barium and strontium (nearly equimolecular ratios); two triple carbonates also formed from mixed crystals of barium, strontium, and calcium (39% CO_3Sr and 4% CO_3Ca). We have also examined simple dioxides of barium and strontium. The sample was heated "by stages" by maintaining it for a certain time at increasing temperatures. For each succeeding stage, we scanned for the masses.

Observation of Ions

Peaks obtained with carbonates. — We will class them into four categories.

1. Background. They are low amplitude peaks corresponding to hydrocarbons. These peaks exist in the absence of carbonates, and even in the absence of binders on the tungsten filament (we have, in fact, investigated the effects of the binder used for the adhesion of the substances). But they are more or less affected by these products as well as by the temperature of the ionic furnace.

We have measured the following peaks: 14, 15, 26, 27, 39-43, 48, 50-57, 62, 64-71, 76-85, 91-93, 95, 97 and 105. One can add water and OH (peaks 18 and 17) as well as residual air.

2. Impurities. They also give low amplitude peaks. Some of these can be masked by the background. In particular, we have found sodium and magnesium (this last metal coming from the binder), as well as impurities from the support. In tests using a nickel support, this metal showed up when sufficiently heated.

3. Gaseous products of carbonate decomposition. We observe an important evolution of carbonic gas indicated by the 44 peak, and also by the 45 and 46 peaks (isotopes), and the 22 peak $(CO_2)^{++}$. If we consider for various carbonates the amplitude of peak 44 as a function of the temperature of the successive stages of "equal duration", we obtain curves similar to that shown in Figure 1. The abscissa I is the current intensity in the furnace filament. The corresponding temperatures were not determined with any accuracy, but the maximum temperature was in the neighborhood of 1800° K. We also note that the release of carbonic gas occurs mostly within a certain temperature interval; the curve allows the determination, in a relative sense, of the total quantity of gas evolved. The position of the maxima depends more or less on the ease with which the decomposition can proceed. In the simple carbonate group, the temperature corresponding to this maximum is clearly lower with calcium carbonate, which is well in agreement with the values for the dissociation pressures [2]. On the other hand, this temperarure is not as high for the double or triple carbonates (mixed crystals) as for the

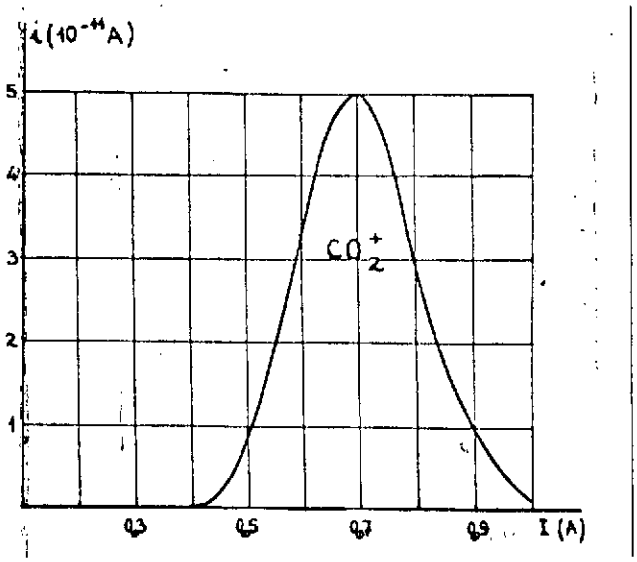

Figure 1.

simple barium carbonate. However, the results can be affected by variations in the residual pressure.

Other peaks appear and give curves similar to the preceding ones. The maximum temperature with each carbonate is approximately the same for all these peaks. We have especially noticed the peaks 12 and 13 (carbon), 16 (oxygen), 28 and 29 (carbon monoxide), as well as peak 32 (molecular oxygen), which is weak. The peaks 12, 16, and particularly 28 are important. They come mainly from the decomposition of carbonic gas. This is mainly spontaneous (and assisted by the high temperature prevailing in the neighborhood of the furnace and of the electron source) or results from electron impact. To obtain an estimate of the ratios of the principal constituents, it is only necessary to consider the amplitude of the various peaks obtained under identical conditions, or to evaluate the "integrals" of the curves (Figure 1). One thus finds the following relative values which are approximately the same for all the carbonates:

C	O	CO	CO_2	O_2
800	1 000	2 400	7 000	1

4. Oxides and products resulting from their decomposition. We have observed the peaks corresponding to BaO (154) and to Ba (138), as well as to SrO (104) and to Sr (88). They are weak, and appear only at the elevated furnace temperatures. The peak of CaO (56) has been detected by pushing the furnace to maximum power, and that of Ca (40) emerges well from the background.

These results must be considered in connection with the activation of the cathodes, particularly in connection with the metallic alkaline earth peaks. For example, one can ask if barium is evaporated directly or, on the contrary, if it results from the electron bombardment of the oxide vapor. However, the results that will be described later concerning the determination of the evolution potentials show that the barium vapor really exists already in the evaporation products. Free barium must effectively be present on the filament coating where it is formed by the reduction, at high

/159

temperature, of the oxide by tungsten and carbon from the binder. Its evaporation is thus related to the "thermal" activation of the oxide, which is obtained without the need for a current to flow through the filament. We have, in fact, simultaneously observed a liberation of oxygen, giving birth to ions that are added to those whose origin was described above.

As far as the oxides are concerned, we know that BaO evaporates more easily than SrO, and SrO more easily than CaO [3]. This order, which our observations have confirmed, seems to be the same for the metals. With carbonates containing barium, we noted that the evaporation rates of this metal are no different, although perhaps a little higher for mixed crystals. It would be interesting to be able to compare the ratios of a metal to its oxide in the evaporation products. According to our results, they seem to be of the same order.

Peaks obtained with the dioxides. We will give only a brief summary of the overall results. Among the impurities we have detected the presence of zinc (64) in barium dioxide, and that of cadmium (112 and 114) in strontium dioxide. The decomposition of dioxides should essentially furnish oxygen: the peaks 16 and 32 are, in fact, important, but we have always observed the peaks 12, 28, and 44, whose existence shows that the dioxides were partially carbonated. We also point out the peak 48, observed with BaO_2.

Direct ion emission by carbonates. We have studied the positive ions emitted by a triple carbonate while the electron source was turned off. Numerous peaks appear when the filament of the ionic furnace is brought to a sufficiently high temperature (2400° K). Some of these must be attributed to alkaline impurities coming from the furnace itself. This could be explained in part by the presence, in the tungsten of the filament, of trace substances constituting the "doping agent" added to the tungsten oxide during fabrication of the metal. As for the alkaline earth metals, they give relatively important peaks. We have obtained ionic current of approximately $2 \cdot 10^{-10}$ amp for barium, a slightly lower value for strontium, and

an order of magnitude 10 times smaller for calcium. The oxide peaks are considerably less well resolved; for BaO the ionic currents were in the neighborhood of $2 \cdot 10^{-13}$ amp, slightly lower for SrO, and not measurable for CaO.

We can also point out that among the most marked is the peak 90, with currents on the order of 10^{-11} amp. The peaks 131, 141, 142, 143, and 144 correspond to currents on the order of 10^{-13} amp. That of CO_2 (44) is the most pronounced. Some of the peaks have an anomalous width, which is probably due to the magnitude and dispersion of the emission velocities of the ions that produce them and for which it would be possible to analyze the "velocity spectrum". The same is also true of the peak 77.

Evolution Potential Measurements of Ions and Study of the Variation in the Effective Ranges of Ionization

The gas molecules are bombarded with electrons having an increasing energy E, and we note, for each mass, the variation in the ionic current i. One can thus determine the "evolution potentials" of the various ions and recognize the variation, with energy E, of the effective ranges of ionization. Moreover, we obtain information concerning the energetic levels of these molecules. The identification of certain ions is made easy by comparing the results with those obtained for cases already known.

The mass spectrograph was used under conditions (recommended by the manufacturer) which permit the reduction to a minimum of parasitic effects. But we are not at all using an impulse method such as that of Fox and his collaborators [4]. We have successively studied a number of gases and, with the ionic furnace, the products evolved from alkaline earth carbonates.

As we shall see, the method of measuring points for i, E curves presents serious disadvantages. In fact, it is often necessary to obtain continuous curves of sufficient accuracy. We have, therefore,

developed an automatic curve tracing method which consists of a recording cylinder whose rotation is coupled to the potential across the electron accelerator.

General shape of the curves. We will begin by examining the "early" portion of the curves, that is, the portion corresponding to energies E not exceeding that of the "threshold" of a few eV at the most. Let us first consider the simple case of a single mode of formation of a given ion. Under these conditions, one readily obtains a curve of the type shown in Figure 2. We distinguish the threshold A, a curved section AB, and a linear part BC. The section AB can only result from the dispersion of the initial electron velocities, which results in the exponential behavior over the interval of 2 to 3 tenths of a volt. In general, to obtain the evolution potential, one extrapolates the linear part down to D on the energy axis. For example, one can account for the initial velocities by adding 0.2 eV to the abscissa of point D. For precise measurements, it is better to use a reference gas such as argon so as to determine the systematic displacements from various sources.

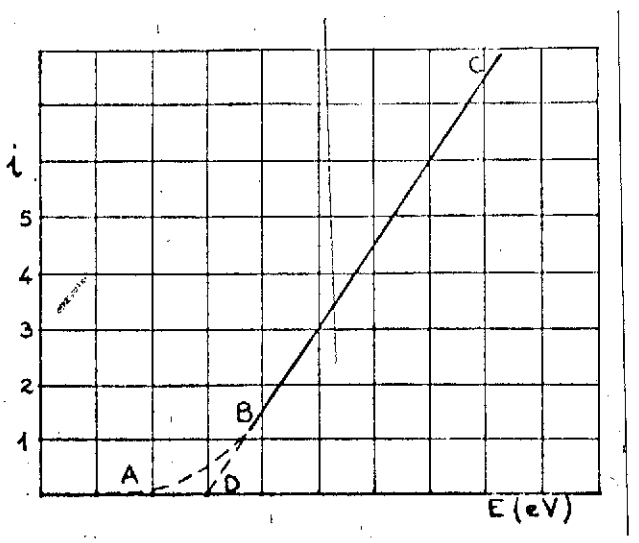

Figure 2

In certain cases, the trace brings out, beyond the threshold, a region of relatively large extent where the variation is approximately parabolic*. When it is followed by a fairly straight section (which is not always the case), the meaning of the extrapolated point D is in doubt. /160

*According to the pulsed results obtained by Fox [4], the linear variation is nevertheless fairly general, but could be perturbed by parasitic effects.

A more complicated and frequent case is that for which, aside from a short initial exponential portion, the trace can be broken down into straight line segments, as shown in Figure 3. It is then necessary to acknowledge the existence of several types of collisions giving birth to ions whose evolution potentials correspond to the intersection or elbow on the trace. If one finds an extended curve of parabolic shape, the interpretation can be very uncertain, because it is often difficult to distinguish a continuous curve of this type from a succession of straight line segments. But in this latter case, one would attempt to deduce from the trace the various values of the evolution potential. If, on the other hand, one recognizes that the curve is really parabolic, one will deduce only one evolution potential whose value is obtained by considering the beginning of the parabola. To improve the accuracy, one traces the straight line representing the variation in $\sqrt{i}$, and extends it until it intersects the energy axis. When there is doubt, it is necessary to state the assumptions used; the parabolic interpretation always leads to an evolution potential slightly lower than the first critical potential obtained (point D) by breaking down the trace into straight line segments. Additional difficulties occur if the trace contains irregularities which can be interpreted, as has been pointed out, as maxima and minima.

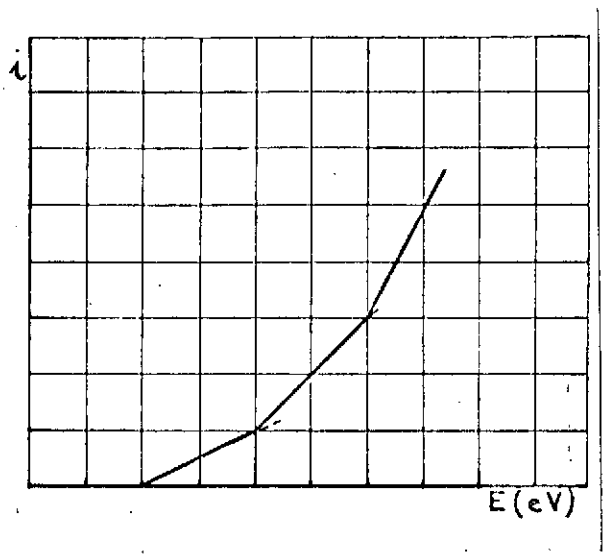

Figure 3.

If one departs from the region of relatively low energies where the first evolution potentials are noticed, the curve represents, except for some corrections, the variation with E of the effective range of ionization. As there exists, in general, several types of collisions whose contributions to the ionic current are comparable, one really observes the sum of these effects, which is, of course, difficult to separate. Our experimental curves thus indicate only

the variation in the "apparent" effective range of ionization, with an arbitrary unit (varying from one case to the other) for the ordinate.

Studies of a few gases. We will briefly present results bearing on a few gases about which we possess precise data, or which have already been investigated by other experimentalists. We have undertaken this study to test the correction of our measurements.

1. Argon. We have found the curve, very often reproduced elsewhere, corresponding to the A^+ ion. For low energies, it matches that of Figure 2, except that section AB is relatively extensive (approximately 2 eV), which can only mean that the electron ejected from the M shell can occupy different energy levels. The evolution potential obtained by extrapolation (point D) is equal to 15.7 $\pm$ 0.1 V, and is in good agreement with known data*. For the A^{++} ion, the curve can be approximated by a parabola over a great distance (Figure 4). The appearance potential is equal to 43.5 $\pm$ 0.5 V, which confirms other recent measurements [5]. For doubly ionized ions of this type, a parabolic variation seems to be the rule [5 - 7], despite a few divergences and attempts at reducing the trace to line segments [8 - 10]. /161

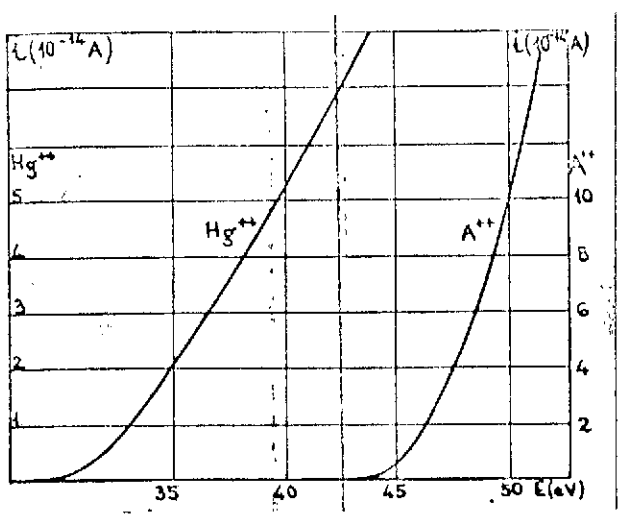

Figure 4

2. Mercury. These peaks come from the mercury vapor used in the pumps. For Hg^+, the case

*Without applying any correction terms, we have most often found values between 15.6 and 15.8 V, and sometimes very near the theoretical value of 15.75 V. In all other cases, the simultaneous investigation of argon has allowed us to determine the origin of the potentials.

is similar to that of Figure 2, with section AB fairly extended. The threshold A corresponds to approximately 9.5 V, and the value of the evolution potential, found by extrapolation, is equal to 10.2 ± 0.2 V. We have not observed, at the corresponding peak, the important irregularities mentioned by other authors [11, 12], although there is a slight manifestation of excited states. With the Hg^{++} ion, we have obtained an evolution potential of 29.5 ± 0.5 V, according to the parabola with which the beginning of the experimental curve of Figure 4 is matched (the method of the straight line would yield a somewhat higher critical potential and would cause another to appear).

3. Nitrogen. The peak 28 of N_2^+ gives a more complicated curve of the type shown in Figure 3. The first evolution potential, equal to 15.6 ± 0.2 V, has long been known. It corresponds to the state $2\sum_{(g)}^{+}$ of the N_2^+ ion. Higher critical potentials relative to the excited states have already been observed: we have found the values of 16.9 ± 0.2 V and 18.8 ± 0.3 V, very close to those found by Fox and Hickman [13], which are related to the $2\prod_{(u)}$ and $2\sum_{(u)}^{+}$ states. Study of the peak 29 (isotope) leads to the same results, but with lower ionic current intensities.

We also observe the peak 14 of the N^+ ion, the evolution potentials of which have been reported by other authors [14 - 16]. The collisions can, in fact, give rise to ions in various excited states which, in particular, can result in the following formation reactions:

$$\begin{array}{l|l} N_2 \rightarrow N(^4S) + N^+(^3P) + e & N_2 \rightarrow N(^4S) + N^+(^1D) + e \\ N_2 \rightarrow N(^2D) + N^+(^1S) + e & e\ N_2 \rightarrow 2\,N^+(^3P) + 2\,e \\ N_2 \rightarrow N^+(^1D) + N^+(^3P) + 2\,e & N_2 \rightarrow 2\,N^+(^1D) + 2\,e \end{array}$$

However, in the region of relatively low potentials, we have clearly distinguished only the values of 24.2 ± 0.3 V, and 26.8 ± 0.4 V (Figure 5).

4. Acetylene. This commercial gas gives a peak 58, whose investigation leads to an evolution potential having a value of 9.8 ± 0.1 V. This peak certainly comes from the acetone in the bottles, and its corresponding critical potential is in good agreement with that of Morrison [17]. The peak 43 is attributable, at least in part, to the CH_3-CO radical that comes from the decomposition of the acetone. The threshold near 10.5 V marks the beginning of a parabolic section followed by a straight line, yielding by extrapolation an evolution potential equal to 13.0 ± 0.3 V.

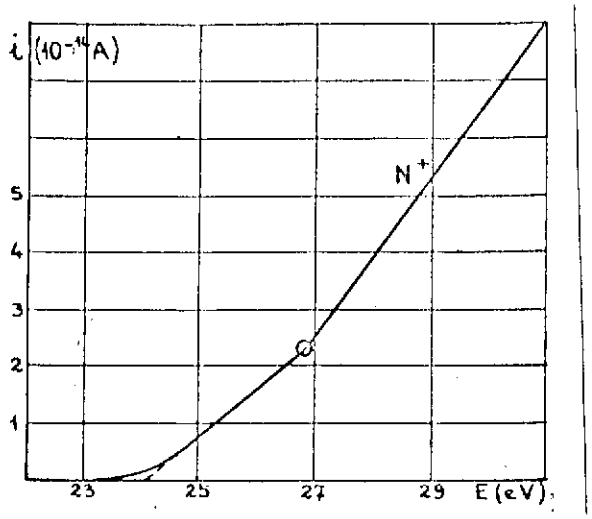

Figure 5

Other peaks are formed by ions produced by carbon and hydrogen. We note in particular the peaks 26 and 27 of $C_2H_2^+$ (C^{12} and C^{13}) with an evolution potential of 11.3 ± 0.2 V; in agreement with earlier results [18, 19]. To the peak 25, due to the C_2H^+ ion resulting from the removal of a hydrogen atom, there corresponds an evolution potential of 17.8 ± 0.2 V, in very good agreement with the results of Tate, Smith and Vaughan [18]. For the three peaks 25, 26, and 27, the amplitude of the curved section of the curve leads to a relatively large displacement between the threshold and the evolution potential. The removal of two hydrogen atoms gives the C_2^+ ion, whose formation is indicated by the peak 24. One finds on its corresponding curve a well defined evolution potential equal to 23.5 ± 0.3 V, already mentioned by Tate, but there seems to exist another one around 20 V (Figure 6).

One also obtains the peaks 15, 14, and 13 for the CH_3^+, CH_2^+, and CH^+ ions, for which the evolution potentials are 15.6 V, 20.8 V, /162

and 22.8 V, respectively, with an uncertainty of 0.1 V, and the threshold potentials are in the neighborhood of 13.5 V, 19 V, and 21 V, respectively. The last value (CH^+) is in agreement with a result of Tate. It seems that trace amounts of nitrogen can contribute to the formation of the peak 14.

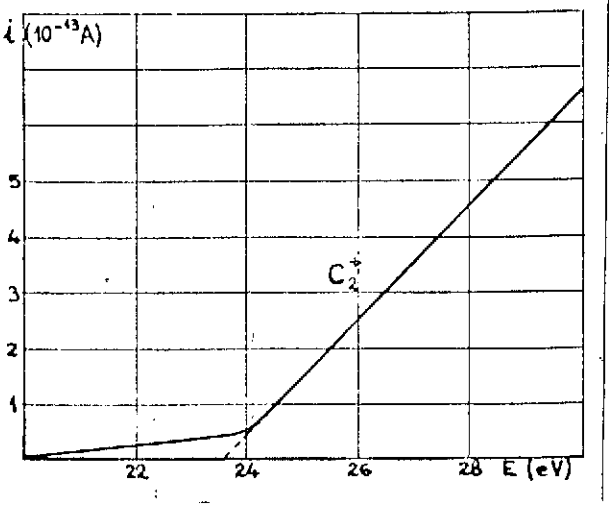

Figure 6

We have also observed the peak 12 due to C^+, for which the curve can be matched to a parabola over a greater part of its length. An evolution potential of 22.0 $\pm$ 0.3 V can be deduced from it. Since the value given by Tate is 24.5 $\pm$ 1 V, it is possible that our value can be attributed to a carbon monoxide process, with the carbonic gas present in trace amounts (the peaks produced by these two gases can be observed). As we shall see, the C^+ ion can be produced in several ways starting from CO and CO_2; the parabolic curve could, in reality, be developed from line segments whose localization is difficult.

On the whole, the results can be affected by some decomposition of the acetylene in the neighborhood of the hot electron source filament.

Study of the Carbonate Evaporation Products with an Ionic Furnace

Aside from facts already known, this study led us to obtain some new results.

1. Carbonic gas and derivatives. The peak 44 gives the curve shown in Figure 7, with a threshold value near 13 V, and with an obvious parabolic section. By extrapolation, it is found that the

evolution potential is equal to 13.9 ± 0.2 V, whereas optical measurement methods [20] give 14.4 V. This difference can be explained by the predissociation, which was observed optically, or by the formation of CO_2 in various vibrationally excited states, which lowers and "spreads" the evolution potential. Our value is, in fact, confirmed by recent measurements made with a mass spectrograph [19, 21, 22]. A slight knee can be seen around 22.5 ± 1 V, and, moreover, we often observe a slight shoulder in the curve in the neighborhood of 19 V. This peculiarity can be simply interpreted by taking account of the optical data relating to the excited states of CO_2 and CO_2^+. The peaks 45 and 46 (isotopes) give identical results. The curve of Figure 8 shows in a more extended interval, the variation in the apparent effective range.

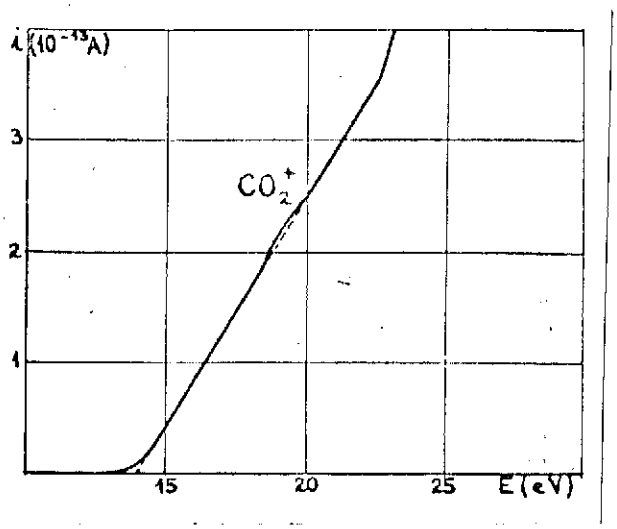

Figure 7

Let us now consider the peak 28 relating to the CO^+ ion which can come from the bombardment of CO_2, and also from the presence of carbon monoxide. According to some measurements [15, 20], the evolution potentials corresponding to these two formation modes would be near 20.4 V and 14 V. More recently, Fox and Hickman [13] performed a detailed analysis of the curve obtained by operating on carbon monoxide. They have deduced evolution potentials of 14 V, 16.4 V, and 19 V that correspond to various states of the CO^+ ion. We have often found these values (the first being obtained by extrapolation with a lower threshold), but sometimes the knees in the curve are observed for other potentials. The peak 28 is thus a complex one because of the various origins of CO^+, and also because of the interaction with residual nitrogen (N_2^+ ions). The curve of effective range (Figure 9) differs little from that mentioned earlier.

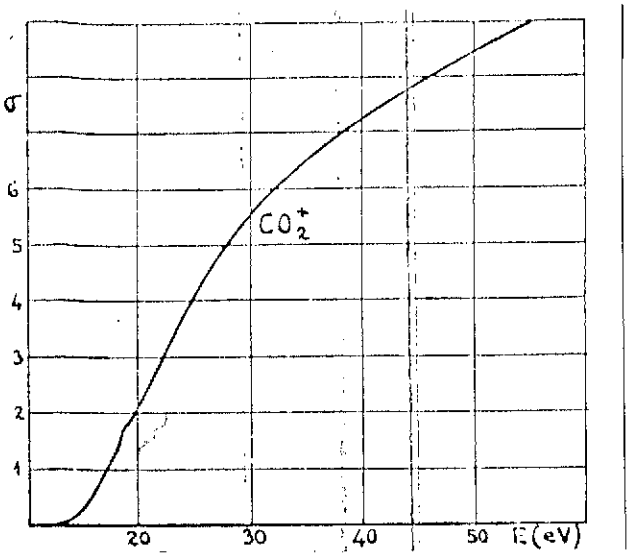

Figure 8

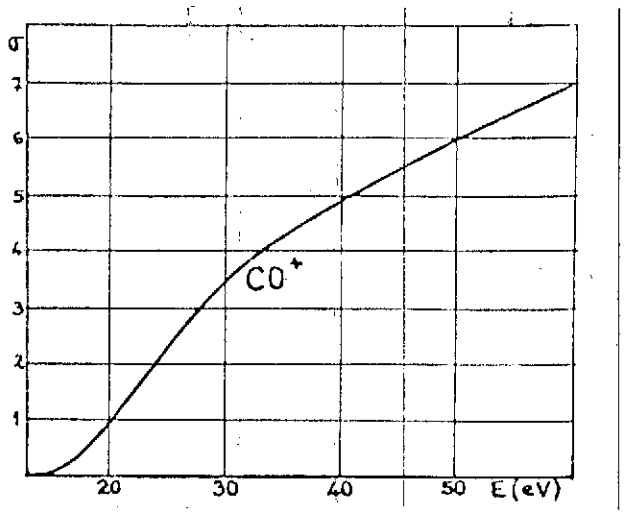

Figure 9

For the peak 22 of CO_2^{++}, the evolution potential is around 38 V, with a fairly large uncertainty (0.6 V). This uncertainty follows from the difficulties in choosing between a very evolved parabola and line segments. Under the latter choice, there would exist another critical potential around 42 V, and perhaps even a higher third one. The variation in the effective range is shown in Figure 10.

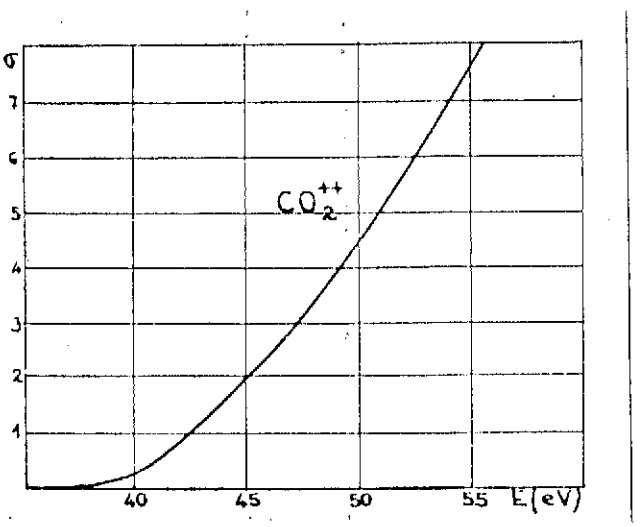

Figure 10

The CO^{++} would yield the peak 14. According to some old measurements [15], the evolution potential would be near 43 V, with a more recent [23] value of 42 ± 0.5 V. In actual fact, it is mostly the N^+ ion of residual nitrogen that contributes to the peak 14, as well as probably other ions such as CH_2^+, because we have sometimes found a first evolution potential abound 19 V. /164

The C^+ ion, which yields the peak 12, can result from the decomposition of CO_2 or CO by electron collision, according to the following process:

$$CO_2 \rightarrow C^+ + 2O + e \quad CO \rightarrow C^+ + O^- \quad CO \rightarrow C^+ + O + e.$$

Old investiations [15, 20, 24] have led to values of little consistency of the evolution potentials relative to the three modes of formation of C^+: approximately 28.5 V starting from CO_2, and 21 V to 23 V starting from CO. For both types of CO decomposition, more recent results [23, 25 - 27] give 21 $\pm$ 0.2 V and 22.8 $\pm$ 0.2 V, respectively. On the whole, our observations confirm these results. As the curve we obtained differs little from a parabola over a wide interval, the precise determination of the critical values is very difficult. It happens that the interaction of CO is negligible because the threshold is then near the highest evolution potential. As far as the variation in the apparent effective range is concerned, one of the curves obtained is that shown in Figure 11.

2. Water and oxygen. Residual water vapor gives rise to the peak 18 which, although not too evident, gives the following precise indications (Figure 12). The evolution potentials are equal to 12.6 $\pm$ 0.2 V, 14.2 $\pm$ 0.4 V, and 16.4 $\pm$ 0.4 V. Numerous earlier

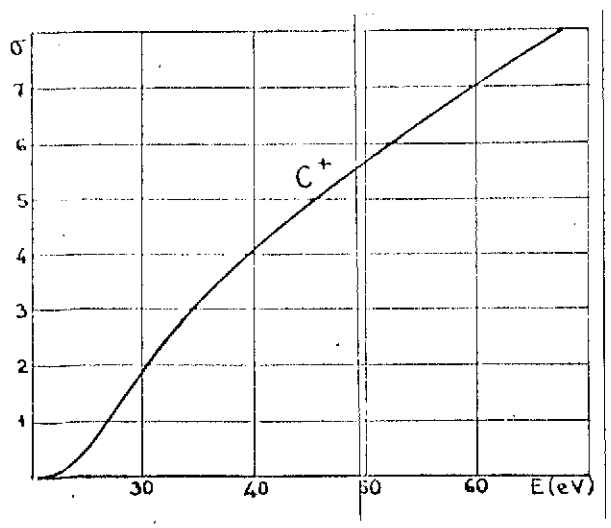

Figure 11

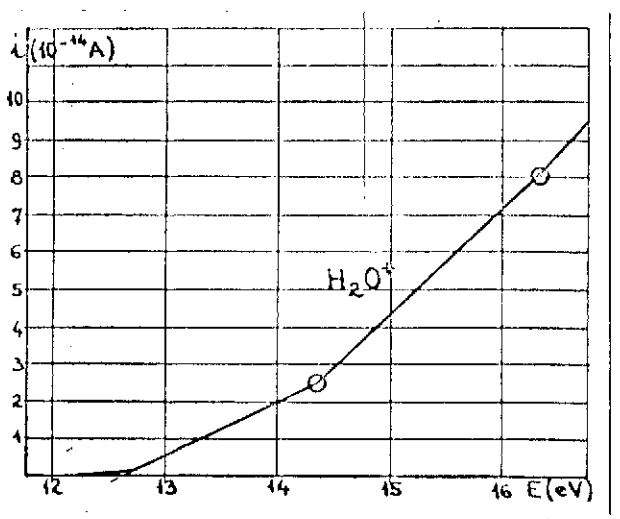

Figure 12

investigations [17, 28 - 39] have led to values of that magnitude. The recent results of Cottin [40] are in good agreement with our own. For the OH^+ ion, the low peak 17 did not lend itself to an accurate analysis. We have found an evolution potential of 17.9 $\pm$ 0.4 V, a value somewhat lower than those of earlier studies, in particular by Smyth and Mueller [30], but in agreement with recent measurements [35, 40]. There also exists another critical potential, rather fuzzy, around 21 V (already noted by Cottin). The curves for the effective range are shown in Figure 13 for these last two ions.

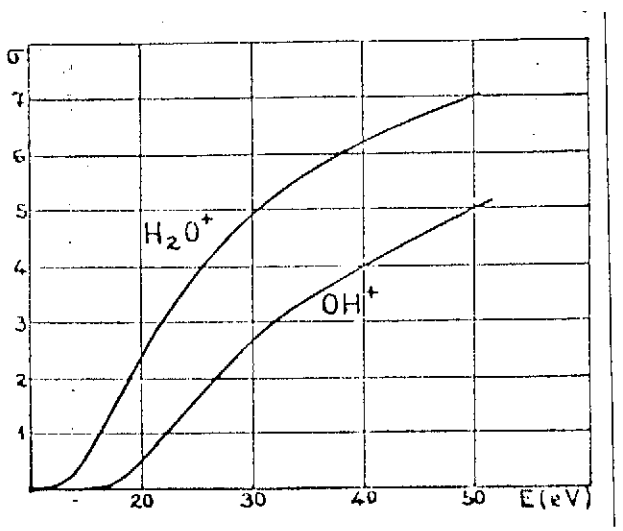

Figure 13

The peak 32, which corresponds to the O_2^+ ion, is complex. The curve obtained is rather near that of a parabola over a wide range, but it seems that it would be possible to consider it as made up of line segments. One should expect to find several evolution potentials. According to some optical measurements, Smyth [20] predicted that one of these, depending on the mode of formation, $2\,CO_2 \rightarrow 2\,CO + O_2$, must be in the neighborhood of 20 V. For the direct ionization of O_2, whose contribution is essential, Mulliken and Stevens [41] have indicated an evolution potential of 12.2 $\pm$ 0.1 V. This value was confirmed later [22, 23, 25, 42 - 45]. However, the excited states of O_2^+ can give rise to other values. We have found a first evolution potential equal to 12.0 $\pm$ 0.3 V; a second one would be near 16 V (15.8 $\pm$ 0.5 V), and there may exist others about 19 V and 23.5 V. The curve shown on Figure 14 indicates the variation of the apparent effective range.

The peak 16, whose amplitude is considerably larger, is produced by the O^+ ion, the various formation modes of which have already been the subject of numerous investigations. An evolution

potential of 19.6 ± 0.4 V for $CO_2 \rightarrow CO + O^+ + e$ has been found [20], whereas the value of 24 V [20] is related to the reaction $CO \rightarrow C + O^+ + e$, and the second value of 23.2 V [25, 27] is related to the reaction $CO \rightarrow C^+ + O + e$. Starting from water vapor, the two formation reactions $H_2O \rightarrow H_2 + O^+ + e$ and $H_2O \rightarrow H_2^+ + O^+ + 2e$ lead, respectively, to the values of 18.5 ± 2 V and 33.5 ± 1 V, according to Smith and Mueller [30].

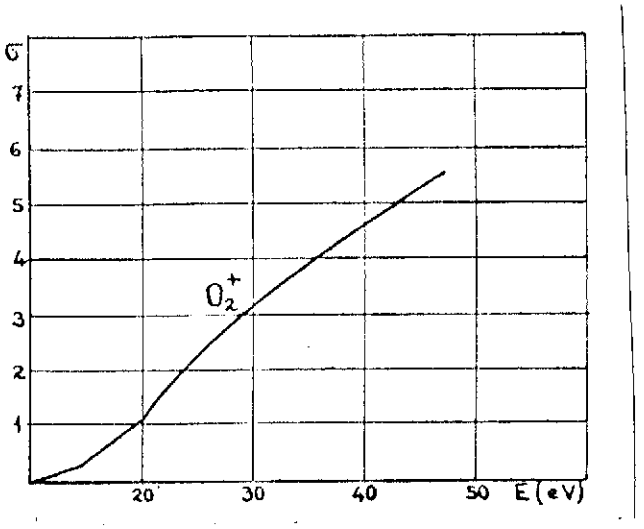

Figure 14

However, for both of these reactions, Mann [34] has obtained 18.8 ± 0.5 V and 28.1 ± 1 V. Concerning the formation under the same conditions of the O^+ ion, Cottin [40] mentions an evolution potential of 29.15 V. As to the production of this ion from molecular oxygen [15, 23, 25, 27, 43, 46], the Table below shows the three reactions considered, the most confident evolution potentials and their calculated values:

$O_2 \rightarrow O^+(^4S) + O(^2P)$ ..	17,0 ± 0,2 V	17,25 V
$O_2 \rightarrow O^+(^4S) + O(^3P) + e$	18,9 ± 0,2 V....	18,69 V
$O_2 \rightarrow O^+(^2D) + O(^2P)$...	20,4 ± 0,2 V	20,57 V

One imagines, therefore, that the traces relating to the peak 16 are very complicated, and that reduction into line segments presents considerable difficulties. However, our measurements are consistent and can be interpreted by taking account of earlier data. The most definite values are located in the neighborhood of 19 V and 23 V. They correspond to the formation of O^+ ions from oxygen and carbon monoxide.

By following the development of the peak 16 during changes in the carbonates, one obtains information about the nature of gases present. Before heating, the peak which is then small is due mainly to the oxygen in the residual atmosphere and water vapor. When heating is moderate, the O^+ ion comes in large part from carbon monoxide and from the oxygen resulting from the decomposition of carbonic gas. Heating to a high temperature allows an evolution potential of about 15 V to be observed, which is lower than any preceding value. This can be attributed to the direct release of the oxygen (in an excited state) from the carbonate or through the interaction of an oxide such as BaO. /165

3. Alkaline earth oxides and metals, and various metals. The curve for BaO is shown in Figure 15, and shows an evolution potential of 6.0 $\pm$ 0.4 V. The evolution potential for SrO, which is clearly higher, could not be determined with any accuracy. In connection with these results, we point out that for these oxides, the dissociation energy has been obtained by various methods [47 - 49]. Values near 5.5 V for BaO and 4.6 V for SrO have been obtained.

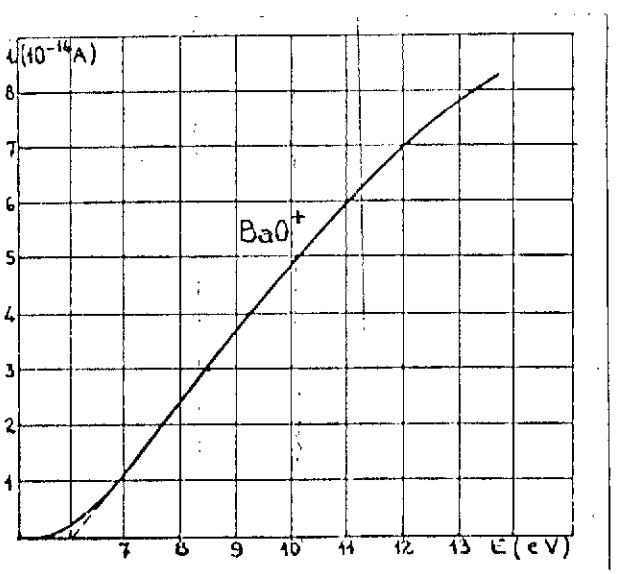

Figure 15

The curves on Figure 16, whose portion near the threshold is very small, show the evolution potential is near 5.35 V for both the Ba^+ and the Sr^+ ions, with an uncertainty of 3 tenths of a volt. These results, in good agreement with optical data, show, for example, that there exists free barium in the evaporation products. The Ba^+ curve of Figure 16 near the low energies shows a maximum followed by a minimum. It is not unusual to observe a maximum in the effective range, but in general it appears at higher energies. Moreover, it is possible

that the trace is perturbed by parasitic effects. However, in this case the minima can be explained, beginning at approximately 11 eV, by another formation mode of the Ba^+ ion, which would then come from the decomposition of BaO. In fact, one obtains about 11 eV by adding 5.3 eV to the dissociation energy of BaO.

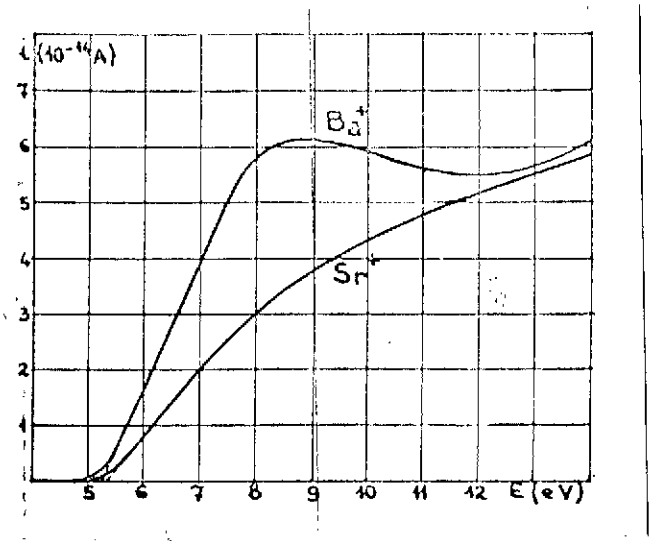

Figure 16

The following evolution potentials were determined for other metals: 8.95 ± 0.1 V from the peaks 112 and 114 of cadmium, 7.5 ± 0.2 V from the peak 24 of magnesium, 7.6 ± 0.2 V from the peaks 58 and 60 of nickel, and 9.3 ± 0.2 V from the peak 64 of zinc. All these values agree with optical data.

4. Miscellaneous peaks. Finally, we have looked at the secondary peaks, which were not all identified. Among these are those constituting the "background" or resulting from the products of decomposition of the binder.

The peak $C_2H_3^+$ (?) gives an evolution potential of 14.9 ± 0.3 V, with a threshold around 14 V. For the peak 30 (CH_2O^+ of $C_2H_6^+$?), this potential is approximately 12 V. The peak 36, with an evolution potential of 12.6 ± 0.2 V should be, according to earlier measurements, attributed to HCl^+ [17, 50]. Values obtained for other peaks are the following: 17.8 ± 0.3 V (peak 48 obtained with barium dioxide), 11.8 ± 0.2 V (peak 67), 9.7 ± 0.3 V (peak 70, probably arising from acetone). The value obtained with the peak 77 is 8.8 ± 0.2 V, which is too small for this peak to be attributable to BaO^{++}.

The results that have been presented show that the study with a mass spectrograph of products liberated by solid substances when heated in vacuum can give useful indications of the changes they undergo in their degree of purity and the nature and the behavior /166 of the evaporation products. In the case of materials used in the manufacture of oxide cathodes, this study can point to the effects of various factors on the activation (carbonates and oxides preparation conditions, type of support, binder composition, impurity content, etc.). On the other hand, the use of this technique can lead to interesting information about the effects of electron bombardment and about the energy levels of some molecules.

REFERENCES

1. Plumlee, R. H. and L. P. Smith. Journ. Applied Physics, Vol. 21, 1950, p. 811.
Aldrich, L. T. J. Appl. Phys., Vol. 22, 1951, p. 1168.
Pelchowitch, I. Phil. Res. Rep., Vol. 9, 1954, p. 42.
Bickel, P. W. and L. V. Holroyd. J. Chem. Phys, Vol. 22, 1954, p. 1793.

2. Hermann, G. and S. Wagener. The Oxide-Coated Cathode, Vol. I., Chapman and Hall, London, 1951, pp. 54-55.

3. Hermann, G. and S. Wagener. loc. cit., pp. 100 - 102.

4. Fox, R. W., W. M. Hickham, T. Kjeldaas and D. J. Grove. Phys. Rev., Vol. 84, 1951, p. 859.

5. Krauss, M., R. M. Reese and V. H. Dibeler. Journ. Res. Nat. Bur. Stand., Vol. 63 A, 1959, p. 201.

6. Wannier, B. Phys. Rev., Vol. 90, 1953, p. 817.

7. Geltman, S. Phys. Rev., Vol. 102, 1956, p. 171.

8. Stevenson, D. P. and J. A. Hipple. Phys. Rev., Vol 62, 1942, p. 237.

9. Hickham, W. M., R. E. Fox and T. Kjeldaas. Phys. Rev., Vol. 96, 1954, p. 63.

10. Fox, R. E. Joint Conf. Mass Spectrometry, London, September, 1958.

11. Nottingham, W. B. Phys. Rev., Vol. 55, 1939, p. 203.

12. Hickham, W. M. Phys. Rev., Vol. 93, 1954, p. 652.

13. Fox, R. E. and W. M. Hickham. Journ. Chem. Phys., Vol. 22, 1954, p. 2059.

14. De Hemptinne, M. and J. Savard. Journ. Phys. Rad., Vol. 6, 1953, p. 499.

15. Vaughan, A. L. Phys. Rev., Vol. 38, 1931, p. 1687.

16. Tate, J. T. and O. W. Lozier. Phys. Rev., Vol. 39, 1932, p. 254.

17. Morrison, J. D. Journ. Chem. Phys., Vol. 19, 1951, p. 1305.

18. Tate, J. T., P. T. Smith and A. L. Vaughan. Phys. Rev., Vol. 48, 1935, p. 525.

19. Honig, R. E. Journ. Chem. Phys., Vol. 16, 1948. p. 105.

20. Smyth, H. D. Rev. Mod. Phys., Vol. 3, 1931, p. 347.

21. Morrison, J. D. Rev. Pure and Appl. Chem., Vol. 5, 1955, p. 22.

22. Warren, J. W., Mass Spectrometry Conf., Institute of Petroleum, London, 1950 - 1952.

23. Hagstrum, H. D. and J. T. Tate. Phys. Rev., Vol. 59, 1941 p. 354.

24. Lozier, O. W. Phys. Rev., Vol. 45, 1934, p. 752; and Vol. 46, 1934, p. 268.

25. Hagstrum, H . D. Rev. Mod. Phys., Vol. 23, 1951, p. 185.

26. Chupka, W. A. and M. G. Inghram. Journ. Phys. Chem., Vol. 55, 1955, p. 100.

27. Hagstrum, H. D. Journ. Chem. Phys., Vol. 23, 1955, p. 1178.

28. Smith, L. G. and W. Bleakney. Phys. Rev., Vol. 49, 1936, p. 883.

29. Price, W. D. Journ. Chem. Phys., Vol. 4, 1936, p. 147.

30. Smyth, H. D. and D. W. Mueller. Phys. Rev., Vol. 43, 1933, pp. 116, 121.

31. Kerwin, L. and M. Cottin. Can. Journ. Phys., Vol. 36, 1958, p. 184.

32. Muschlitz, E. E. and T. L. Bailey. Journ. Phys. Chem., Vol. 60, 1956, p. 681.

33. Cox, B. C. Thesis, Liverpool, 1953.

34. Mann, M. M., A. Hustrulid and J. T. Tate. Phys. Rev., Vol. 58, 1940, p. 340.

35. Foner, S. N. and R. L. Hudson. Journ. Chem. Phys., Vol. 25, 1956, p. 602.

36. Frost, D. and C. A. McDowell. Can. Journ. Chem., Vol. 36, 1957, p. 39.

37. Lindeman, L. P. and J. C. Cuffy. Journ. Chem. Phys., Vol. 29, 1958, p. 217.

38. Morrison, J.D. Journ. Chem. Phys., Vol. 19, 1951, p. 1305.

39. Price, W. C. and T. M. Sugden. Trans. Faraday Soc., Vol. 44, 1948, p. 108.

40. Cottin. Journ. Chimie Physique, Vol. 56, 1959, p. 1024.

41. Mulliken, R. and D. Stevens. Phys. Rev., Vol. 44, 1933, p. 720.

42. Marriott, J. Thesis, Liverpool, 1954.

43. Thorburn, R. Appl. Mass Spectrometry, Institute of Petroleum, London, 1954, p. 185.

44. Smith, S. J. and L. M. Branscomb. Journ. Res. Nat. Bur. Stand., Vol. 55, 1955, p. 165.

45. Waldron, J. D. and K. Wood. Mass Spectrometry Conf., Institute of Petroleum, London, 1950 - 1952.

46. Tate, J. T. and P. T. Smith. Phys. Rev., Vol. 39, 1932, p. 270.

47. Huldt, L. and A. Lagerquist. Ark. Fys., Vol. 2, 1950 p. 333.

48. Brewer, L. and D. F. Mastick. UCRL Report No. 533, University of California, 1949.

49. Drummond, G. and R. F. Barrow. Trans. Faraday Soc., Vol. 47, 1951, p. 1275.

50. Nier, A. O. and E. E. Hanson. Phys. Rev., Vol. 50, 1936, p. 722.

Translated for National Aeronautics and Space Administration under contract No. NASw 2483 by SCITRAN, P. O. Box 5456, Santa Barbara, California, 93108